# Assessing Connections in Networks of Biological Neurons

David R. Brillinger*and Alessandro E.P. Villa†

*The stronger the qualitative understanding the data analyst can get of the subject-matter field from which his data comes, the better - just so long as he does not take it too seriously.*

Mallows and Tukey (1982)

**Abstract**

In this work spike trains of firing times of neurons recorded from various locations in the cat's auditory thalamus are studied. A goal is making inferences concerning connections amongst different regions of the thalamus in both the presence and the absence of a stimulus. Both second-order moment (frequency domain) and full likelihood analyses (a threshold crossing model), are carried through.

## 1 Introduction

The sequence of spikes of a neuron, referred to as a "spike train", may carry important information processed by the brain and thus may underlie cognitive functions and sensory perception [1]. The data studied are recorded stretches of point processes corresponding to the firing times of

*Statistics Department, University of California, Berkeley
†Institute of Physiology, University of Lausanne, Switzerland

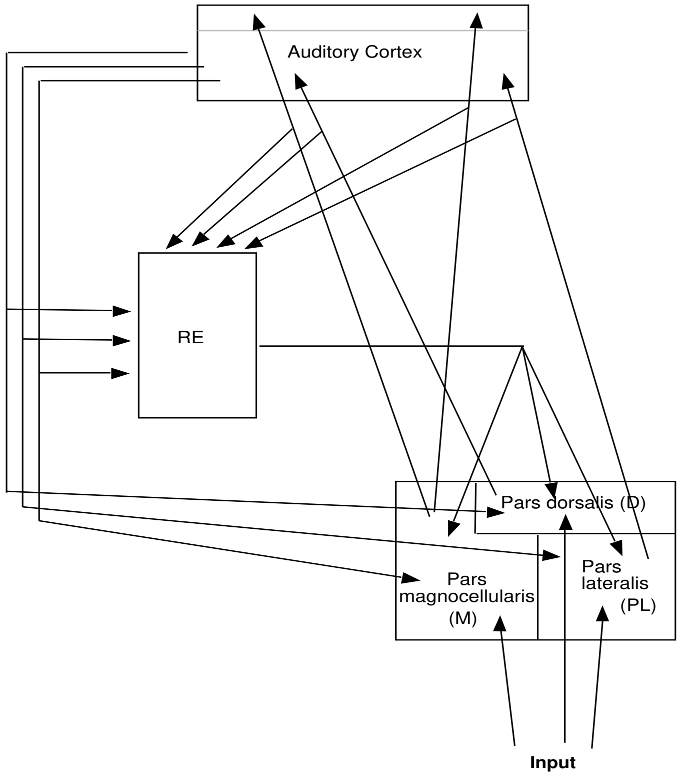


Figure 1: A block diagram of the auditory regions of the cat's brain.

neurons measured in the cat's auditory thalamus [25]. This set of nuclei is often viewed as the penultimate in an ascending hierarchy of processing stages of the auditory sensation that begins at the level of the inner ear. The thalamic nuclei belonging to the cat auditory pathway are the *medial geniculate body* ($MGB$), the lateral part of the thalamic posterior complex and the *reticular nucleus of the thalamus* ($R$ or $RE$). The $RE$ receive and send projections to the other thalamic subdivisions through an array of convergent and divergent connections [22]. Figure 1 provides a block diagram indicating some plausible connections amongst the regions of the auditory system of concern in this work.

A basic goal of the paper is to obtain some understanding of how auditory regions of the brain interact. More specifically, results are presented about the association of *pars magnocellularis* ($M$) of the medial geniculate body and the reticular nucleus of the thalamus. Special interest has been raised by these thalamic subdivisions because $M$, also known as the medial division of $MGB$, is characterized by a unique pattern of projection to all the auditory cortical fields [17, 19] and $R$ is playing a key-role in the adaptive filtering of the auditory input to the cerebral cortex [23].

The data were collected during two recording conditions: a first in which the neurons were firing spontaneously, a second in which white noise sound bursts were applied regularly as a stimulus. The simultaneous recording of the electrophysiological activity of neurons in $R$ and $M$ was replicated, at times separated by 2 to 8 hours, between successive experiments. One interesting problem involved in this study is how to combine the results of different recording sessions.

Two types of analyses are presented in the paper. The first is based on second-moment statistics in the frequency domain, while the second is based on a conceptual (threshold crossing) model for neuron firing. Previous work on the problem of interacting neurons includes: [2, 13]. This paper continues the work of [9, 6].

# 2 Experimental Background

The experiment was conducted in a nitrous-oxide anesthetized young adult cat in compliance with Swiss guidelines for the care and use of laboratory animals and after receiving governmental veterinary approval. The experimental procedure and ordinary time series analysis of this dataset are described in [21]. Briefly, the anesthesia was induced by an intra-peritoneal injection of sodium pentobarbital (Nembutal, 40 mg/kg body weight). The cat was mounted in a stereotaxic instrument and a small hole was trepanated on the skull, at the level of the auditory thalamus. The anesthesia during the recording sessions was maintained by an artifical ventilation with a mixture of 80% $N_2O$ and 20% $O_2$. The reflex state, pupil size and blood pressure were monitored in order to detect any sign of discomfort of the cat.

Extracellular single unit recordings were made with glass-coated platinum-plated tungsten microelectrodes having an impedance in the range 0.5-2 M$\Omega$ measured at a frequency of 1 kHz. Up to six microelectrodes could be advanced independently. The dataset analyzed here was collected from one electrode inserted in $R$ (2 spike trains) and two electrodes inserted in $M$ (3 spike trains). Simultaneous recording of spike trains from the same microelectrode was achieved by using an analog template matching spike sorter according to a technique described elsewhere [14, 22]. The firing times were measured by a microcomputer with an accuracy of 1 ms and stored digitally for off-line analysis. The activity of a group of units was recorded during 40 to 60 minutes. Four recording sessions, performed at intervals of 2 to 8 hours, involving three units in $M$ and two units in $R$ are used to assess the connections between these thalamic subdivisions.

Several stimuli were applied in order to characterize some typical response properties of auditory units, but the results reported in this paper were collected in two recording conditions: during stimulation by a white noise burst (at an intensity of 72 dB *sound pressure level* delivered to both ears simultaneously) at a frequency of 1 stimulus/second (i.e. lasting 200 msec followed by 800 msec of silence) and during absence of external stimulation, to be referred to as *spontaneous activity*. The spike trains were collected during 5 to 8 minutes of each recording condition.

Figure 2 provides raster plots of the data for five neurons of one of the recording sessions involving stimulation. Each dot represents the occurrence of a spike. Here in an individual raster plot, spike times for 300 successive repetitions of the stimulus presentation are stacked above each other, aligned on the stimulus onset. For unit (neuron) 1, one sees a solid transient response to the stimulation a brief latency after the beginning of stimulus application. For unit 4, one can note a transient increase of activity after a longer latency than observed in unit 1 followed by an increase of activity lasting up to the ending of the noise burst.

Upon completion of the experiment, an electrolytic lesion was performed at a known depth for each microelectrode track, by passing a current of about 8 $\mu$A during 10 s. At the end of the recording session the animal received a lethal dose of Nembutal, and the brain was prepared for standard histological procedures. These allowed the physical locations of the neurons recorded to be obtained.

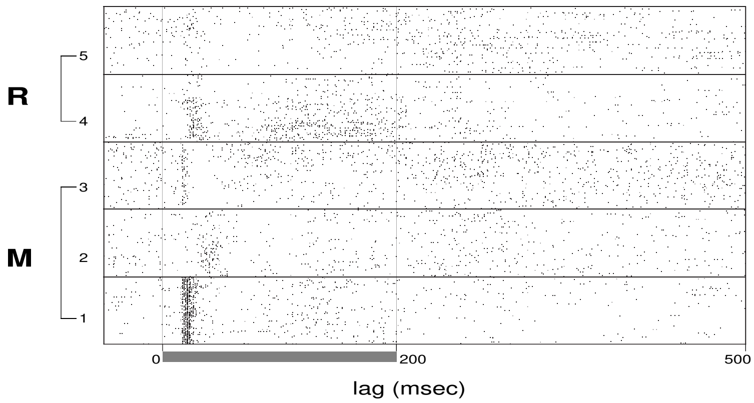


Figure 2: Raster plots of experiment w21q04 with stimulation. The gray bar indicates the presence of the stimulus. A pair of units 1, 2 and unit 3 were recorded in $M$ subdivision of MGB from two microelectrodes, respectively, and a pair of units 4, 5 was recorded in $R$.

# 3 Statistical Background

Two distinct types of analyses are presented. The first is a second-order moment analysis working with multivariate statistics computed in the frequency domain. The second is a likelihood analysis based on a conceptual model for the firing of a neuron. In the second case, the parameters are estimated by the method maximum likelihood.

## 3.1 Second moment analysis based on FTs

The points of a pair of contemporaneous of point processes, $M$ and $N$, may be denoted $\sigma_m$, $m = 0, \pm 1, \ldots$ and $\tau_n$, $n = 0, \pm 1, \ldots$ respectively. The data may be thought of as a segment of a realization of a bivariate stationary point process. The empirical Fourier transform of the $\sigma$ points is

$$d_M^T(\lambda) = \sum_m e^{-i\lambda\sigma_m} \tag{1}$$

where $T$ denotes the length of the time period of observation and for $\lambda$ real-valued. Under conditions of stationarity and mixing such Fourier transforms often satisfy central limit theorems. The *coherency* of the $M$ and $N$ processes, at frequency $\lambda$, may be defined as

$$R_{MN}(\lambda) \;=\; lim_{T\to\infty} corr\{\sum_m e^{-i\lambda\sigma_m},\ \sum_n e^{-i\lambda\tau_n}\} \tag{2}$$

Its modulus-squared the *coherence*, $|R_{MN}(\lambda)|^2$, is a measure of the linear time invariant dependence of the two processes at frequency $\lambda$, see eg. [3]. One way to see the reasonableness of these definitions is to consider the case of ordinary time series whose components take on the values $0-1$. With fine enough time interval expression (1) corresponds to the usual Fourier transform of a stretch of such $0-1$ values.

A measure of conditional dependence of processes $M$ and $N$, given some other processes is provided by the *partial coherency*

$$R_{MN|rest} \;=\; (R_{MN} \;-\; R_{M|rest}\bar{R}_{N|rest})/\sqrt{(1\;-\;|R_{M|rest}|^2)(1\;-\;|R_{N|rest}|^2)} \tag{3}$$

having supressed the dependence on $\lambda$. Here $R_{MN}$ is given by (2), while

$$R_{M|rest}(\lambda) \;=\; lim_{T\to\infty} corr\{\sum_m e^{-i\lambda\sigma_m},\ B^T(\lambda)\}$$

with $B^T(\lambda)$ denoting the best (minimum mse linear) predictor of (1), excluding the process $N$. Estimates of the coherence and partial coherence may be based directly on empirical Fourier transforms of the point processes involved. For example, one could take

$$\hat{R}_{MN}(\lambda) \;=\; \frac{\sum_l d_M^T(\lambda,l)\overline{d_N^T(\lambda,l)}}{\sqrt{\sum_l |d_M^T(\lambda,l)|^2 \sum_l |d_N^T(\lambda,l)|^2}} \tag{4}$$

with the sums over $l \;=\; 1,...,n$ empirical Fourier transforms of the form (1) based on separate time stretches. For another estimation method see [3, 7].

Examples of partial coherence computations for networks of three neurons may be found in [7]. Other neurophysiological examples may be found in [18]. References on partial coherence in the time series case include [4, 12, 20].

For the data sets of interest, the neurons fall into particular regions of the brain and it is desired to have measures of the strengths of connection amongst pairs of these regions. This necessitates a form of multivariate analysis. The particular regions studied here are $M$ and $R$, as sketched in Figure 1.

The fact that the empirical Fourier transforms are approximately Gaussian, suggests employing some traditional procedure of multivariate (Gaussian) analysis. Let $\hat{\mathbf{R}}$ refer to the matrix of sample coherencies computed for all available neurons (either in region $M$ or region $R$.) (Again dependence on $\lambda$ is being suppressed.) Let $\hat{\mathbf{R}}_{MM}$ and $\hat{\mathbf{R}}_{RR}$ refer to submatrices of $\hat{\mathbf{R}}$ corresponding to the $M$ units and $R$ units, respectively. The $|.|$, in (5) below, denotes the determinant of the matrix involved with the dependence on $\lambda$ suppressed for simplicity's sake. A test of independence of the $M$ and $N$ components can be based on the likelihood ratio or deviance statistic

$$-2\ n\ log\{|\hat{\mathbf{R}}|/|\hat{\mathbf{R}}_{MM}||\hat{\mathbf{R}}_{RR}|\} \tag{5}$$

approximating its null distribution by a chi-squared with degrees of freedom $2p_M p_R$. In the case of independence, for the population values,

$$|\mathbf{R}| \ = \ |\mathbf{R}_{MM}||\mathbf{R}_{RR}|.$$

The $p_M$ and $p_N$ denote the numbers of rows in $\hat{\mathbf{R}}_{MM}$ and $\hat{\mathbf{R}}_{RR}$ respectively and $n$ is the number of time segments in an estimate such as (4). (Here $p_M p_N$ complex parameters have been set to 0 under the null hypothesis of independence of the $M$ and $R$ regions, hence the indicated degrees of freedom.) More accurate approximations to the distribution of (5) are suggested in [24, 15].

Independent experiments may be combined by adding the statistic (5) over experiments, with a corresponding addition of degrees of freedom. This will be the case for the example in Section 4.

When stimulation is present, to assess connections independent of stimulation, one might work with the coherencies having "partialled out" the point process of stimulus application times. To do so one proceeds as in (3), but for example replacing $\hat{\mathbf{R}}_{MM}$ by

$$\hat{\mathbf{R}}_{MM} \ - \ \hat{\mathbf{R}}_{\mathbf{MS}}\hat{\mathbf{R}}_{\mathbf{SS}}^{-1}\hat{\mathbf{R}}_{\mathbf{SM}}$$

The values of such a statistic will be presented in Section 4.

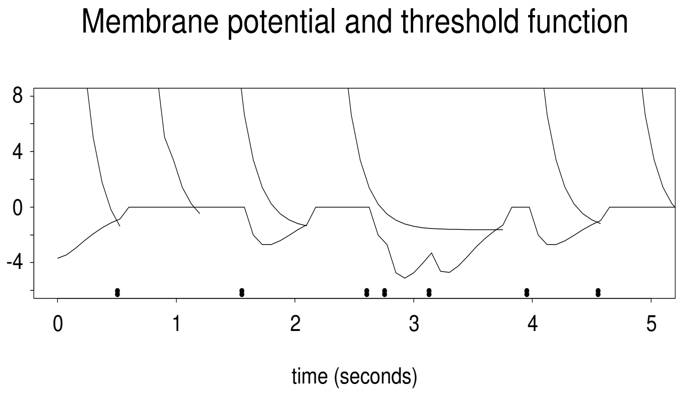


Figure 3: The functions $U(t)$, $\theta(t)$ and input spike times.

## 3.2 Likelihood analysis of a conceptual model

Brillinger and Segundo, [8], introduce maximum likelihood fitting of a *threshold crossing* model for a neuron firing as a function of input. Suppose that firing of the neuron takes place when an internal state variable, $U(t)$ the *membrane potential*, upcrosses a (random) threshold $\theta(t)$. The value $U(t)$ will depend on the inputs received by the cell. It will be assumed that the threshold is reset after firing, which in effect introduces a refractory period. Figure 3 provides a graph of the functions $U(t)$ and $\theta(t)$ for one case. The piles along the time-axis indicate input neuron spike firing times. The j-shaped curves correspond to $\theta(t)$. Output firings occur at the times when $U(t)$ and $\theta(t)$ meet. In the case of this figure, the input is inhibitory as seen by the dipping of $U(t)$ after the arrival of an input spike.

Consider a neuron, $M$, driving a neuron, $N$. In the fitting of the threshold model it is convenient to replace the point process values by $0-1$ valued discrete time series values, taking a fine time interval. Define

$$M_t \; = \; 1 \quad \textit{if spike in the interval } (t, t+1]$$

and $M_t = 0$ otherwise for $t = 0, \pm 1, \ldots$ and some small time interval. There is a similar definition for $N_t$. If $\gamma_t$ denotes the time since the neuron $N$ last fired, the membrane potential will be approximated by

$$U_t \; = \; \sum_{u=1}^{\gamma_t} m_{t-u} M_u$$

for some *summation* function $m_t$. It will be further assumed that

$$\theta_t \; = \; d \; + \; e\gamma_t \; + \; f\gamma_t^2 \; + \; g\gamma_t^3 \; + \; \epsilon_t \tag{6}$$

with the $\epsilon_t$ independent standard normals. The cubic form is employed here to be able to produce $J$-shaped threshold forms and as a form linear in the unknown parameters. Taking $\Phi$ for the standard normal cumulative the log likelihood, given the input, is

$$\sum_t [N_t \; log \; \Phi(U_t - \theta_t) \; + \; (1 - N_t) \; log(1 \; - \; \Phi(U_t - \theta_t))]$$

In the example to be presented parameter estimates will be determined by maximizing this expression. Results of such a fitting, in the case of single input and output spike trains or of spike train output with noise input, may be found in [8, 5].

For the experiments of interest a multivariate version of the model is needed. There will be an arbitrary number of neurons, situated in several regions of the brain. Also a stimulus will be present during particular time intervals. Define a stimulus variable by setting $S_t \; = \; 1$ whilst the stimulus is applied and $S_t \; = \; 0$ otherwise. Then for the $j-th$ neuron one can consider a model with $N_{j,t} \; = \; 1$ when

$$\alpha S_t \; + \; \sum_{k \neq j} \sum_{u=1}^{\gamma_{jt}} a_{jk,t-u} N_{k,u} \; > \; \theta_{j,t} \tag{7}$$

and $N_{j,t} \; = \; 0$ otherwise, $t \; = \; 0, \; \pm 1, ...$ and $\theta_{j,t}$ given by (6) and $\gamma_{jt}$ is the time elapsed since neuron $j$ last fired. The $j-th$ and $k-th$ neurons may be in the same or different regions of the brain.

To assess the hypothesis that some of the $a_{jk,.}$ are identically 0 one can compute the change in the deviance (- twice the log-likelihood), occurring when the hypothesis is incorporated. This quantity may be viewed as a measure of the strength of the connection, see [6]. Examples of this and estimates of the $a_{jk,.}$ are presented in the next section.

# 4 Results

The regions of the brain, for which results are presented in this paper, are $M$, the *pars magnocellularis*, and $R$ (or $RE$), the *reticular nucleus* of the thalamus. Questions of interest include: Is there association of regions $R$ and $M$? Are there direct connections of R and M? Is apparent association due to signal driving? How strong are the connections? The results of the analyses are presented next.

## 4.1 Second-order Analysis

Figure 4 provides the values of the mod-square of the statistic (4) in the cases of stimulation (upper panels) and of spontaneous firing (lower panels), and also the corresponding partial coherence "removing" the effects of stimulation as in (3). The dashed line provides the approximate upper 95% null line, based on the approximating chi-squared distribution. The degrees of freedom were summed over 4 cell groups and totalled 48 here. One sees low frequency association in each case. The upper left graph shows strong association around 1.8 Hz and apparent association up to about 15 Hz. Note that no major peaks were observed on either condition at frequencies higher than 25 Hz. The upper right panel of Figure 4 shows the overall association much reduced, when the linear time invariant effects of the stimulus are "removed". There is an intriguing peak in the two top graphs at 7.9 Hz. The bottom two graphs are much the same, as they should be. In a sense the upper right graph is meant to estimate the lower left. (Up to sampling variation this would be precisely so if the relationship was linear.)

One would like to say that there is association at very low frequencies independent of the stimulation. Association near 7.9 Hz appears only during the stimulus condition, but it was apparently not linearly locked to the stimulus onset, as suggested by the persistence of the peak at 7.9 Hz in the estimate of the partial 'stimulated' coherence (Figure 4, upper right panel). However, it needs to be noted that, more than 5% of the points of the panel are above the 95% null line. The spike train recordings of the four groups were carried out at different times. The excess of points here may be the consequence of a time trend or some other individual experimental effect.

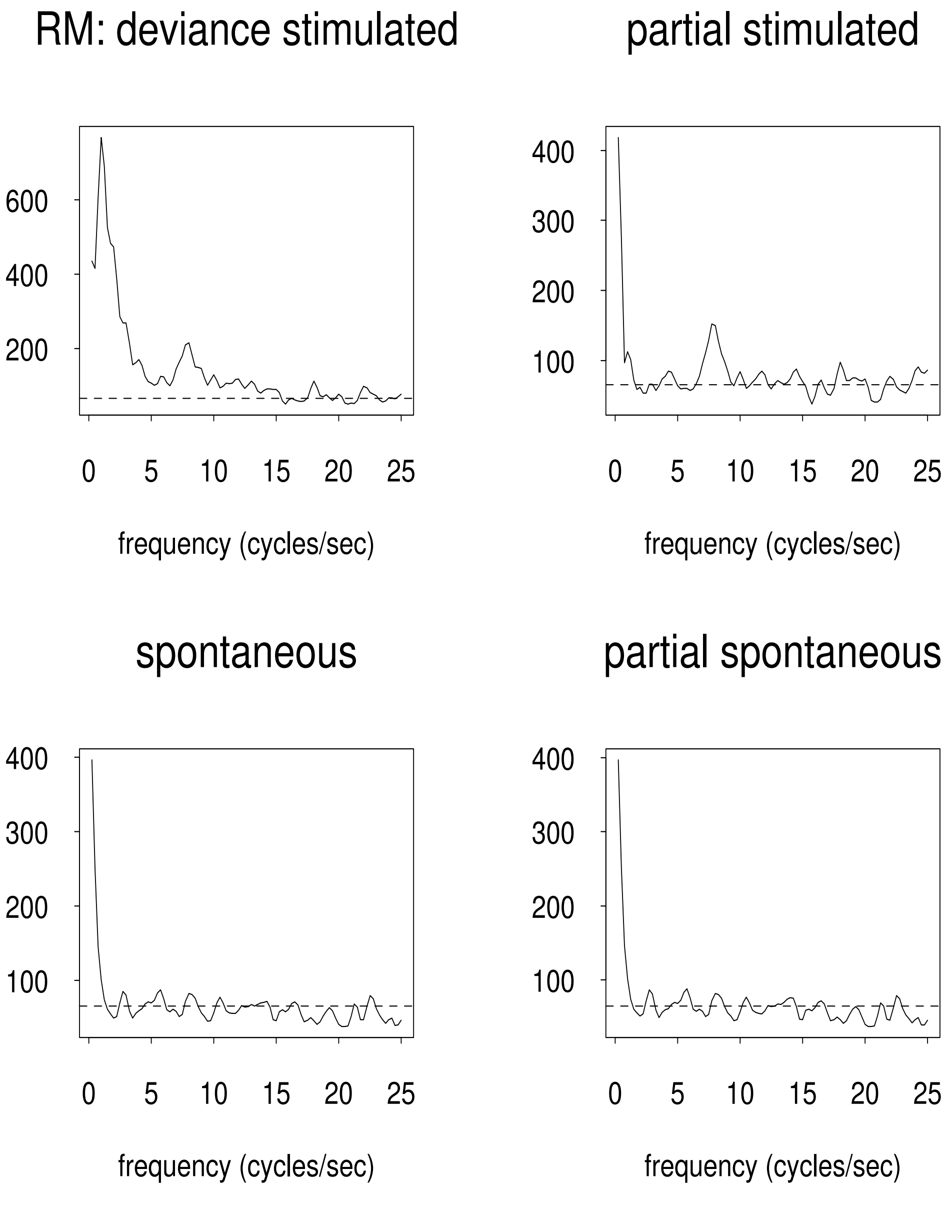


Figure 4: The statistic (4) summed over four recording sessions.

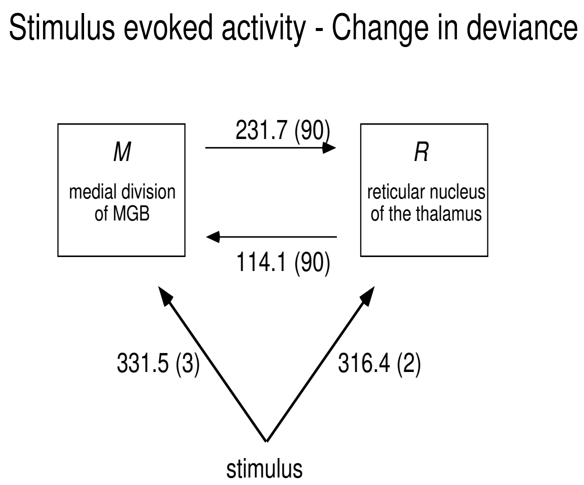


Figure 5: Deviance differences for the likelihood fits. Degrees of freedom in (.) .

## 4.2 Likelihood analysis

Figure 5 displays the results of fitting the model (7) and in particular the changes in deviance when the arrows concerned are removed from the diagram. The experiments are the same as in Section 4.1. The results are combined by adding the deviances. The figures in brackets are the degrees of freedom of a null chi-squared statistic. It is clear that there is a strong association with the stimulus in each case. The direct connection from $M$ to $R$ appears stronger than the reverse, if one takes deviance as a measure of strength of association.

In the case of a single recording session it is possible to show the estimated $a_{jk,\cdot}$. Figure 6 shows the neurons recorded in the first recording session and the estimated functions $a_{jk,\cdot}$ of the model (7). The upper left panel provides the summation function for the influence of the second neuron of $R$ on the first in the presence of the neurons of M.

The remaining panels on the left refer to the influence on the first neuron of $R$ of the 3 neurons of $M$. The right column similarly refers to the second neuron of $R$. To put it in other words, the left column refers to R1 being influenced by R2, M1, M2, M3 and the right to R2 being influenced by R1,

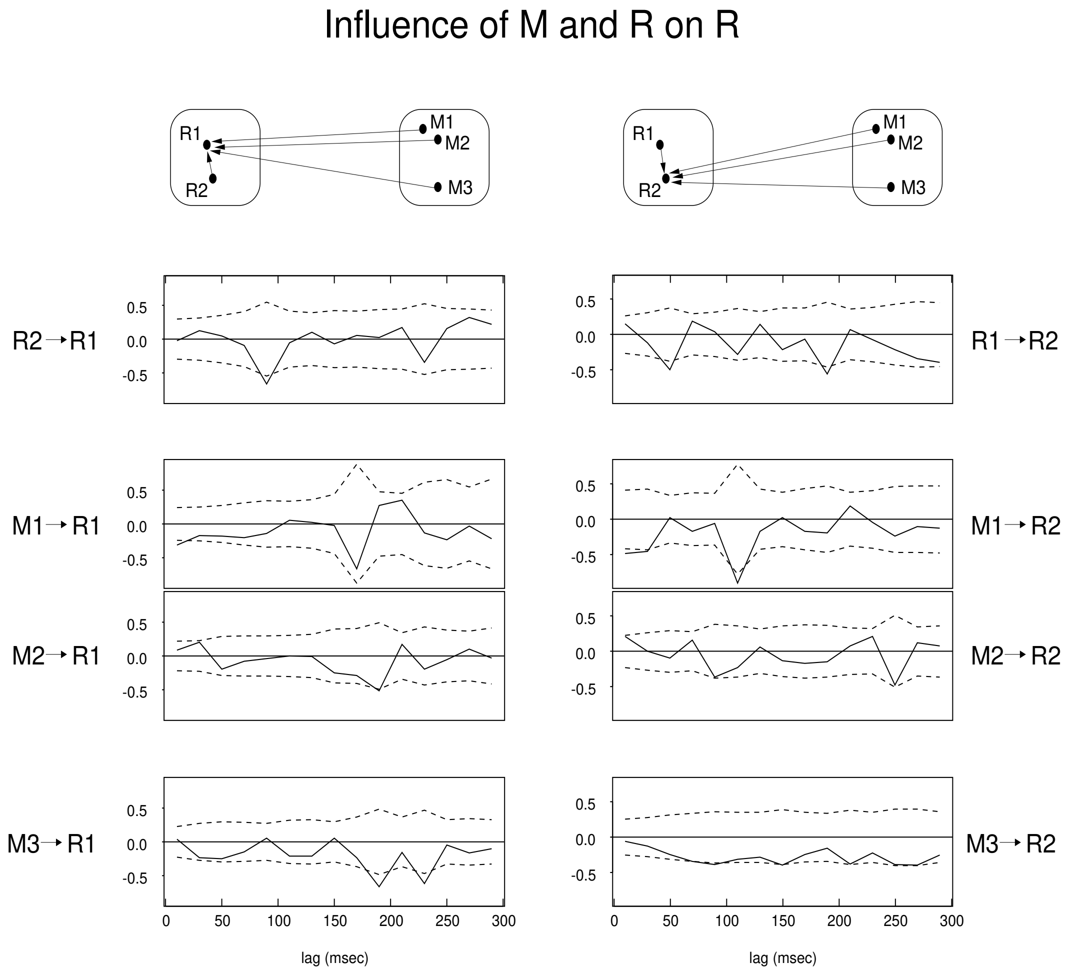


Figure 6: The left column provides influences on neuron R1 from other neurons of R and those of region M. In the top panel, arrows indicate the considered directions of influence. The right column similarly refers to R2.

M1, M2, M3. Note that discharges of cell pair $R1$ and $R2$ were recorded simultaneously from the same electrode. Units $M1$ and $M2$ were also recorded from the same, but different than the previous, electrode. The dashed lines give approximate $\pm 2$ standard error limits. The standard errors are approximate, computed by the usual maximum likelihood formulas. While for the three experiments merged the influence of M on R appeared substantial (deviance of 231.7 with 90 degrees of fredom), none of the summation function estimates (for the first experimen alone) appears strongly significant. Further investigations are being carried out. Perhaps the standard errors are inappropriate. Perhaps there are lurking correlations.

A problem is how to combine such $\hat{a}_{jk,\cdot}$ for several experiments. The difficulty is that different neurons and paths are involved, hence for example different latencies of effect may occur.

# 5 Discussion and Summary

As indicated at the outset, the goal was to make inferences concerning connections amongst regions of the auditory thalamus, both in the presence and absence of a stimulus. Here the work has been on the *reticular nucleus of the thalamus* and *pars magnocellularis* of the medial geniculate body. Two methods for investigating the wiring diagram of a particular point process system have been presented and illustrated. A second-moment analysis showed the usefulness of the study of frequency bands and provided a global estimation of the strength of the connections between the regions under study. A likelihood approach was based on the basic biology. One interesting feature of this method is the possibility to elaborate detailed inferences on the temporal pattern of the connections. This may represent a fundamental clue for understanding the information processing carried out by these regions in the thalamus. Both methods proved convenient for combining the results of different experiments. Uncertainty measures were central to making inferences.

There are a number of difficulties that arise in this work. The data are numerous and of complex structure. A neuron may receive thousands of inputs and data are available for but a few. The sampling of the regions of the brain cannot be expected to be unbiased. An approach needs to be developed that reduces the influence of individual neurons on the statistics computed in case something unusual is taking place for one of them. Nonstationarity and experiment effects are sometimes present. Recent evidence of non-linear deterministic dynamics in spike trains, as indicated by the apparent existence of low-dimensional chaotic attractors [10, 11], should also taken into account for global estimations of cumulated recording sessions. Thus, it appears that future work will look for the evolution of the system in time. This also represents a necessary step for applying these methods to neurophysiological data about learning and memory.

## 6 Acknowledgements

Some may have been intrigued by the Mallows-Tukey quote at the head of the article. The remark is highlighted because one of us, as a graduate student, remembers JWT making remarks such as: "To consult with a chemist, you have to become a chemist." We thank Stefan Morgenthaller for helpful comments on the manuscript.

The authors would like to acknowledge the support of U.S. grants of the National Science Foundation DMS-9300002 and DMS-9625774 and the Office of Naval Research Grant ONR-N00014-94-1 and of the Swiss National Science Foundation Grant 31-37723.93.

## References

[1] Abeles, M. (1991). Corticonics: neural circuits of the cerebral cortex. Cambridge University Press, Cambridge, UK.

[2] Borisyuk, G.N. (1985). A new statistical method for identifying interconnections between neuronal network elements. Biological Cybernetics 52, 301-306.

[3] Brillinger, D.R. (1975). The identification of point process systems. Annals of Probability 3, 909-929.

[4] Brillinger, D.R. (1975). Time Series: Data Analysis and Theory. Holt Rinehart, New York.

[5] Brillinger, D.R. (1992). Nerve cell spike train data analysis: a progression of technique. J. American Statistical Assoc. 87, 260-271.

[6] Brillinger, D.R. (1996). Remarks concerning graphical models for time series and point processes. Revista de Econometria, 16, 1-23.

[7] Brillinger, D.R., Bryant, H.L. and Segundo, J.P. (1976). Identification of synaptic interactions. Biological Cybernetics 22, 213-228.

[8] Brillinger, D.R. and Segundo, J.P. (1979). Empirical examination of the threshold model of neuron firing. Biological Cybernetics 35, 213-220.

[9] Brillinger, D.R. and Villa, A.E.P. (1994). Examples of the investigation of neural information processing by point process analysis. Pp. 111-127 in Advanced Methods of Physiological System Modelling 3 (ed. V.Z. Marmarelis), Plenum, New York.

[10] Celletti, A. and Villa, A.E.P. (1996) Low dimensional chaotic attractors in the rat brain. Biological Cybernetics 74, 387-394.

[11] Celletti, A. and Villa, A.E.P. (1996) Determination of chaotic attractors in the rat brain. J. of Statistical Physics 84: 1379-1386.

[12] Gersch, W. (1972). Causality or driving in electrophysiological signal analysis. Mathematical Bioscience 14, 177-196.

[13] Gerstein, G.L., Perkel, D.H. and Dayhoff, J.E. (1985). Cooperative firing activity in simultaneously recorded populations of neurons: detection and measurement. J. Neuroscience 5, 881-889.

[14] Ivarsson, C., De Ribaupierre, Y. and de Ribaupierre, F. (1988). Influence of auditory localization cues on neuronal activity in the auditory thalamus of the cat. J. Neurophysiology 59, 586-606.

[15] Krishnaiah, P.R., Lee, J.C. and Chang, T.C. (1983). Likelihood ratio tests on covariance matrices and mean vectors of complex multivariate normal populations and their applications in time series. Pp. 439-476 in Handbook of Statistics 3 (eds. D.R. Brillinger and P.R. Krishnaiah). North-Holland, Amsterdam.

[16] Mallows, C.M. and Tukey, J.W. (1982). An overview of the techniques of data analysis, emphasizing it exploratory aspects. Pp. 111-172 in Some Recent Advances in Statistics (Eds. T. de Oliviera et al.) Academic, New York.

[17] Morel, A. and Imig, T.J. (1987). Thalamic projections to fields A, AI, P, VP in cat auditory cortex. Journal of Comparative Neurology 265, 119-144.

[18] Rosenberg, J.R., Amjad, A.M., Breeze, Brillinger, D.R. and Halliday, O.M. (1989). The Fourier approach to the identification of functional coupling between neuronal spike trains. Progress in Biophysics and Molecular Biology 53, 1-31.

[19] Rouiller, E.M., Rodrigues-Dagaeff, C., Simm, G., de Ribaupierre, Y., Villa A.E.P. and de Ribaupierre, F. (1989). Functional organization of the medial division of the medial geniculate body of the cat: tonotopic organization, spatial distribution of response properties and cortical connections. Hearing Research 39, 127-142.

[20] Tick, L.J. (1963). Conditional spectra, linear systems and coherency. pp. 197-203 in Time Series Analysis (ed. M. Rosenblatt). Wiley, New York.

[21] Villa, A.E.P. (1988) Influence de l'écorce cérébrale sur l'activité spontanée et évoquée du thalamus auditif du chat, Presses Imprivite, Lausanne.

[22] Villa, A.E.P. (1990). Functional differentiation within the auditory part of the thalamic reticular nucleus of the cat. Brain Research Review 15, 25-40.

[23] Villa, A.E.P., Rouiller, E.M., Simm, G.M., Zurita, P., de Ribaupierre, Y. and de Ribaupierre, F. (1991). Corticofugal modulation of the information processing in the auditory thalamus of the cat. Experimental Brain Research 86, 506-517.

[24] Wahba, G. (1971). Some tests of independence for stationary time series. J. Royal Statistical Soc. B 33, 153-166.

[25] Webster, D.B., Popper, A.N. and Fay R.R. (1992). The Mammalian Auditory Pathway. Springer Verlag, New York.